Appl. Phys. A (2016)122:881
DOI 10.1007/s00339-016-0419-7

Applied Physics A
Materials Science & Processing

Shield gas induced cracks during nanosecond-pulsed laser irradiation of Zr-based metallic glass

Hu Huang[1] · Jun Noguchi[1] · Jiwang Yan[1]

Received: 30 June 2016 / Accepted: 2 September 2016

Abstract Laser processing techniques have been given increasing attentions in the field of metallic glasses (MGs). In this work, effects of two kinds of shield gases, nitrogen and argon, on nanosecond-pulsed laser irradiation of Zr-based MG were comparatively investigated. Results showed that compared to argon gas, nitrogen gas remarkably promoted the formation of cracks during laser irradiation. Furthermore, crack formation in nitrogen gas was enhanced by increasing the peak laser power intensity or decreasing the laser scanning speed. X-ray diffraction and micro-Raman spectroscopy indicated that the reason for enhanced cracks in nitrogen gas was the formation of ZrN.

1 Introduction

In recent years, laser processing techniques, such as selective laser melting (SLM) [1–3], laser welding [4, 5], laser cladding [6–8], laser ablation [9–11], laser deposition [12, 13], and so on [14, 15], have been given increasing attentions in the field of metallic glasses (MGs). Laser processing exhibits the potential to solve some critical problems in the applications of MGs [1], especially the limitation of product size. For example, laser welding [4, 5] can join small MGs to form a bigger one, and thus it can enlarge the product size of MGs. SLM, as an emerging additive manufacturing technique, potentially provides an alternative method to prepare large MGs from MG powders [3]. Furthermore, SLM can fabricate complex geometries free of using expensive molds, satisfying more complex or customer-designed applications [1, 3]. Laser deposition can form MG coatings with increased hardness, wear, and corrosion resistance on crystal substrates, providing a new application method of MGs [16].

During laser processing, shield gases such as argon and nitrogen [1] are commonly used to avoid oxidation and crystallization of MGs. Previous studies [3, 4, 7, 12] were focused on evolution of the structure and mechanical properties of MGs before and after laser processing, and efforts were made to keep the properties unchanged. However, up to date, there are few studies on the effects of shield gases on the laser processing of MGs. Although shield gases do not react with MGs at ambient temperature and pressure, chemical reactions might be activated when MGs are in complex states such as molten, vaporized, and boiled states during nanosecond-pulsed or shorter pulsed laser irradiation [9]. In this case, new phases may be generated on the irradiated surface of MGs. In this paper, we report comparative experiments of nanosecond-pulsed laser irradiation of Zr-based MG in nitrogen and argon shield gases, which demonstrate that shield gases significantly affect the laser irradiation process, and thus induce different surface characteristics.

2 Material and experiments

$Zr_{41.2}Ti_{13.8}Cu_{12.5}Ni_{10}Be_{22.5}$ MG samples (commonly called Vitreloy 1) with a diameter of 10 mm and thickness of 2 mm were cut from a rod-like as-cast MG using a low speed diamond saw, and then, the slices were mechanically polished using 400, 800, and 1500 grit sand papers in sequence. Laser irradiation was performed using a

✉ Jiwang Yan
yan@mech.keio.ac.jp

[1] Department of Mechanical Engineering, Faculty of Science and Technology, Keio University, Yokohama 223-8522, Japan

Published online: 08 September 2016

Nd:YAG nanosecond-pulsed laser system (LR-SHG, MegaOpto Co., Ltd., Japan) with a wavelength of 532 nm and pulse width of 15.4 ns. The laser beam was shaped to a square of ~85 μm × 85 μm, and the laser pulse frequency was kept 1 kHz. Various scanning speeds (1, 5, 10 mm/s) and peak laser power intensities (1.3×10^{12}–5.3×10^{12} W/m^2) were selected. Two commonly used shield gases, nitrogen and argon, were used for comparison, and the gas pressure was the same (0.05 MPa). Because the size of a single MG sample was not enough to complete all experiments, laser irradiation was done on two MG samples. For each sample, laser power was re-calibrated using a laser power meter.

Morphologies of the laser irradiated regions were observed by a digital microscope (VHX-1000, Keyence, Japan), a three-dimensional (3D) laser scanning microscope (VK-9700, Keyence, Japan), and a scanning electron microscope (SEM) (Inspect S50, FEI, USA). Surface characteristics of the MG before and after laser irradiation were characterized by an X-ray diffractometer (XRD, D8 Discover, Bruker, Germany) and a micro-Raman spectroscopy (NRS-3100, JASCO, Japan).

3 Results and discussion

Figure 1 presents SEM morphologies of irradiated regions after single-line laser scan under different shield gases [(a) and (b) argon gas; (c) and (d) nitrogen gas]. All the other experimental conditions were exactly the same, i.e., the peak laser power intensity of 1.4×10^{12} W/m^2 and scanning speed of 1 mm/s. Figure 1a and c show the surface morphologies in the center region of single-line laser scan, and Fig. 1b and d show the morphologies at the end point. In Fig. 1c, remarkable cracks are observed around the irradiated region, and they become clearer at the end point of the irradiated region in Fig. 1d. Furthermore, line-like microstructure appears on the side of irradiated region in Fig. 1c. However, only very small cracks are observed in Fig. 1b, and it is nearly featureless in the center region as

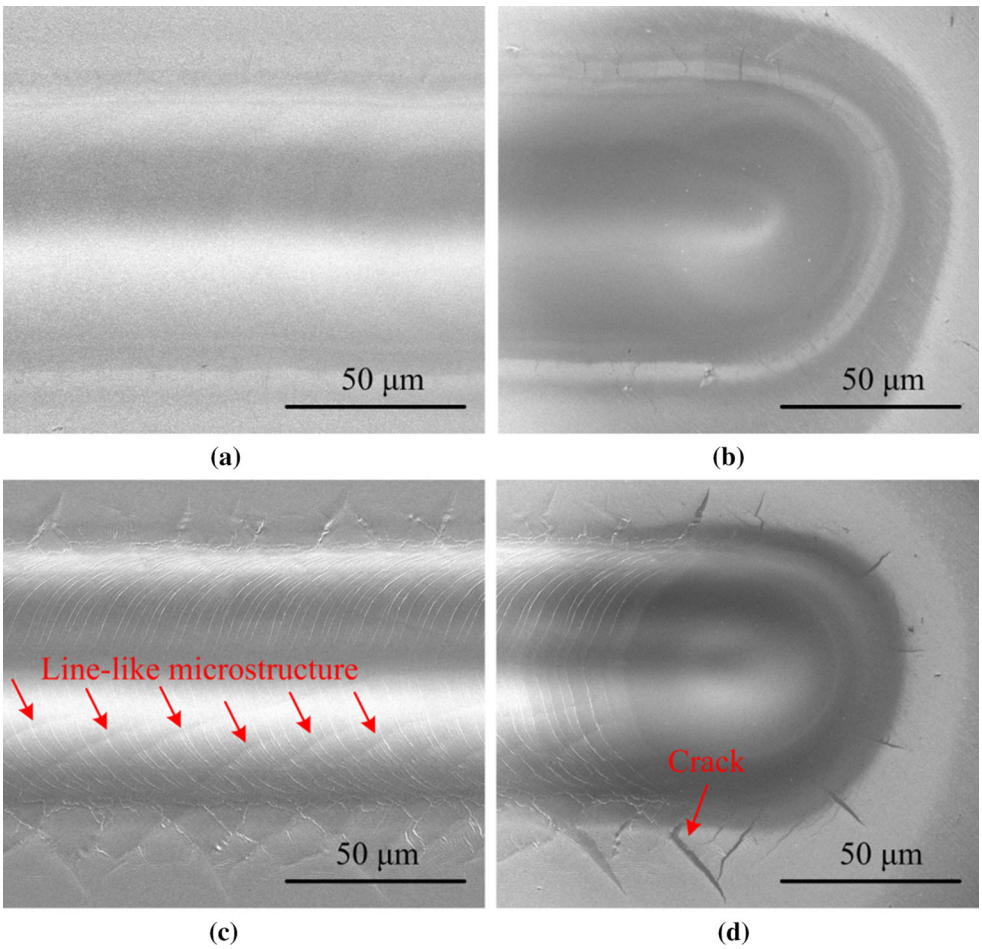

Fig. 1 SEM morphologies of *single-line* laser irradiated regions under a peak laser power intensity of 1.4×10^{12} W/m^2 and a scanning speed of 1 mm/s: **a**, **b** argon shield gas; **c**, **d** nitrogen shield gas

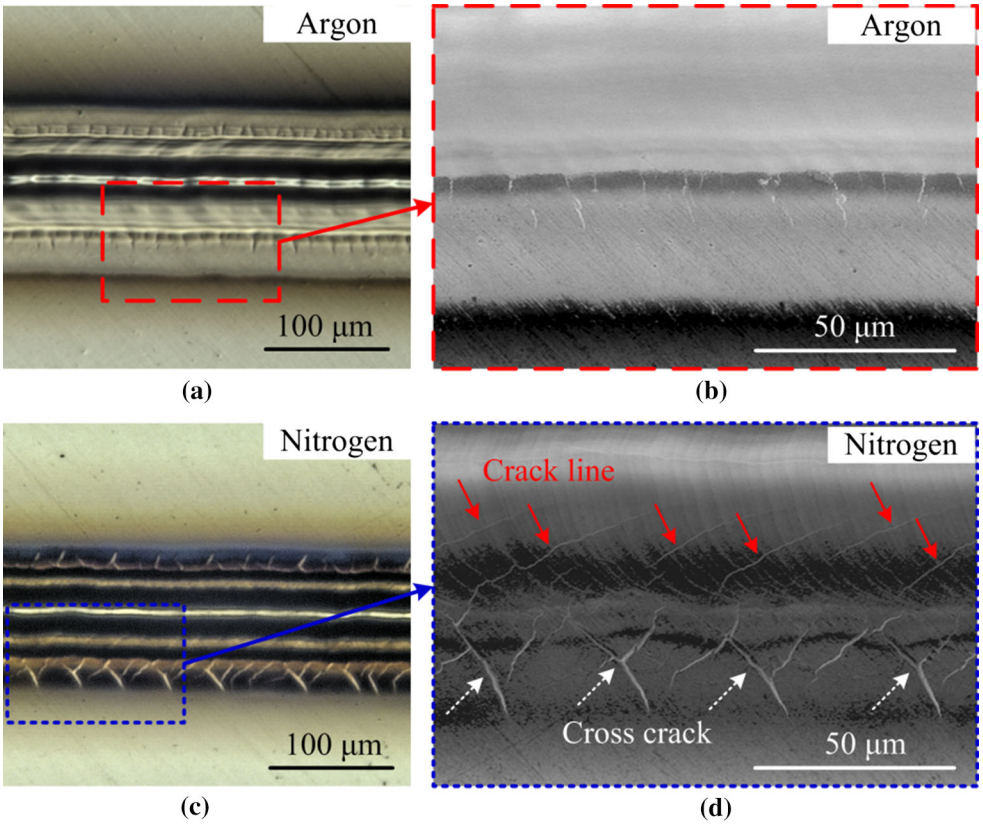

Fig. 2 Optical morphologies of *single-line* laser scan in the center regions, corresponding to the SEM morphologies in Fig. 1a and c

shown in Fig. 1a. The comparative results in Fig. 1 indicate that nitrogen shield gas induces remarkable cracks, while argon shield gas nearly does not induce cracks during nanosecond-pulsed laser irradiation of Zr-based MG.

To further investigate the line-like microstructure in Fig. 1c and confirm the difference in crack in Fig. 1, Fig. 2 presents optical morphologies of single-line laser scan in the center regions, corresponding to the SEM morphologies in Fig. 1a and c, respectively. Taking a high contrast of the optical microscope, cracks are visually enhanced in Fig. 2 compared to those in Fig. 1. In Fig. 2a and b, small cracks are also observed around the irradiated regions. Similar to those in Fig. 1c, remarkable cross cracks are clearly observed in Fig. 2c and d. According to the morphology in Fig. 2d, the line-like microstructure in Fig. 1c is confirmed to be cracks.

To study effects of the peak laser power intensity and scanning speed on crack formation as well as subsequent scans on previously formed cracks, multi-line laser scans were performed under increased peak laser power intensities and various scanning speeds with an overlapped region of 45 μm between two scanning lines. Figure 3 presents typical SEM morphologies at the ends of multi-line laser scanned regions. For irradiation in nitrogen shield gas, the increased scanning speed obviously suppresses crack formation as shown in Fig. 3a–c. Compared to the cracks in Fig. 1d, the morphology at the end point in Fig. 3a shows slightly enhanced cracks when the peak laser power intensity increased to 3.4×10^{12} W/m^2. However, for irradiation in argon shield gas, no obvious cracks are observed in SEM morphologies under the increased peak laser power intensity and scanning speeds (Fig. 3d presents an example). In Fig. 3a–c, it is also noted that subsequent laser scans gradually healed the cracks formed in previous scans. Accompanying with the formation of laser irradiated regions, heat-affected zones (HAZs) were also generated around the irradiated regions as shown in Fig. 1b and d. The previous laser scan was in the HAZ of the subsequent laser scan, and the MG materials in the HAZ have an enhanced flow ability [17]. Thus, with the role of recoil pressure generated by vaporization of MG materials in the irradiated region, some previously formed cracks which were in the HAZ of the subsequent laser scan could be healed by further material flow.

Although the absorbed laser energies by the MG surface were different because of various energy losses when the laser beam penetrated various shield gases, the comparative results in Figs. 1 and 3 under various peak laser power intensities and scanning speeds exclude this reason that leads to the enhanced cracks in nitrogen shield gas, and

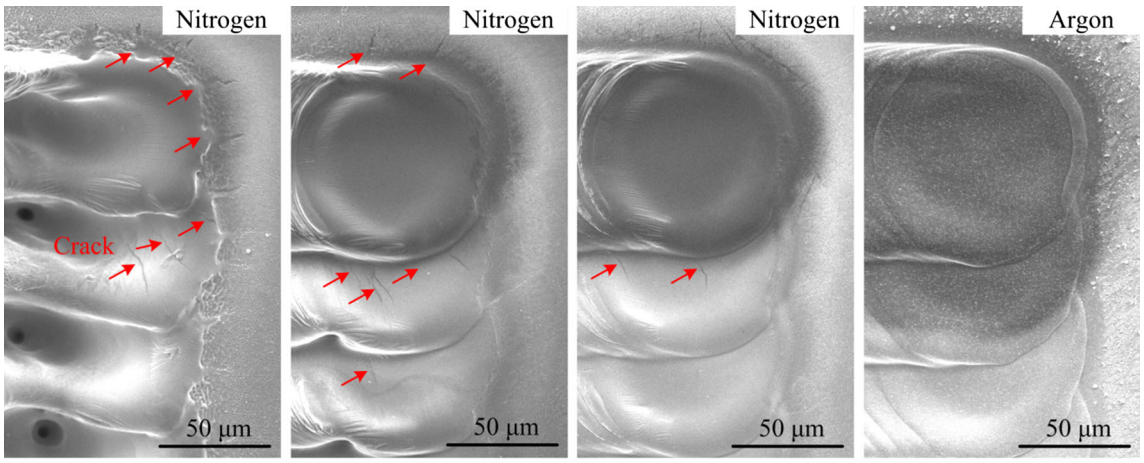

(a) 1 mm/s **(b)** 5 mm/s **(c)** 10 mm/s **(d)** 5 mm/s

Fig. 3 SEM morphologies at the ends of *multi-line* laser scanned regions under an increased peak laser power intensity of 3.4×10^{12} W/m^2 and various scanning speeds

other reasons exist. To further explore possible reasons leading to the formation of remarkable cracks during laser irradiation of Zr-based MG in nitrogen shield gas, surface characteristics of the multi-line laser scanned regions were characterized by XRD and micro-Raman spectroscopy, and results are illustrated in Fig. 4. Experimental conditions are inserted in each figure. In Fig. 4a, although all XRD patterns show a broad hump under the scanning speed of 1 mm/s, some small sharp peaks appear which correspond to cubic ZrN according to the XRD software. Furthermore, with increase in the peak laser power intensity, these sharp peaks are slightly enhanced. For a constant peak laser power intensity of 3.4×10^{12} W/m^2, the increased scanning speed suppresses the appearance of ZrN peaks. Results in Fig. 4a and b indicate that the formation of ZrN in Zr-based MG during laser irradiation in nitrogen shield gas is affected by the peak laser power intensity and scanning speed. A high peak laser power intensity and low scanning speed promoted the formation of ZrN. However, in Fig. 4c, for the regions irradiated in argon shield gas, there is no obvious crystal peak under a low scanning speed of 1 mm/s and various peak laser power intensities. Raman spectra in Fig. 4d further confirm this difference obtained in different shield gases. There is nearly no difference between the Raman spectra obtained in the regions irradiated in argon shield gas and the as-cast surface. However, for the regions irradiated in nitrogen shield gas, two peaks appear in their Raman spectra, which are related to the formation of nitride according to Ref. [18].

Previous studies [2] suggested that cracks formed during laser irradiation in argon shield gas are mainly attributed to the thermal mismatch between the molten layer and substrate, which leads to high stress at their interface during solidification of the molten layer at high cooling rate because of thermal contraction and solidification shrinkage. This can be used to explain the formation of very weak cracks around the irradiated regions in argon shield gas in Fig. 2a. By comparatively analyzing XRD patterns and Raman spectra in Fig. 4, it is clear that the remarkable cracks formed during nanosecond-pulsed laser irradiation of Zr-based MG in nitrogen shield gas result from the formation of ZrN. The ZrN has a thermal expansion coefficient of 7.2×10^{-6} K^{-1} [19], and it is 8.8×10^{-6} K^{-1} for the Vitreloy 1 MG [20]. The newly formed ZrN embedded in MG matrix enhances the thermal mismatch between the molten layer and substrate, and thus, cracks were enhanced during nanosecond-pulsed laser irradiation of Zr-based MG in nitrogen shield gas. Additionally, the consistency of the slightly enhanced cracks in Fig. 3 and the enhanced ZrN peaks in XRD patterns in Fig. 4a and b under an increased peak laser power intensity or a decreased laser scanning speed further confirms the role of ZrN for formation of enhanced cracks in nitrogen shield gas. Under an increased peak laser power intensity or a decreased laser scanning speed (more accumulated heat), more MG materials are liquidized and vaporized, and thus more ZrN is expected to be generated. Accordingly, enhanced ZrN peaks and cracks are observed.

4 Conclusions

In summary, effects of nitrogen and argon shield gases on nanosecond-pulsed laser irradiation of Zr-based MG were comparatively investigated. Results indicated that compared to argon gas, nitrogen gas remarkably promoted the formation of cracks. Furthermore, with increase in the peak laser power intensity or decrease in the laser scanning speed, crack formation during laser irradiation in nitrogen gas was enhanced. In multi-line laser scans, subsequent

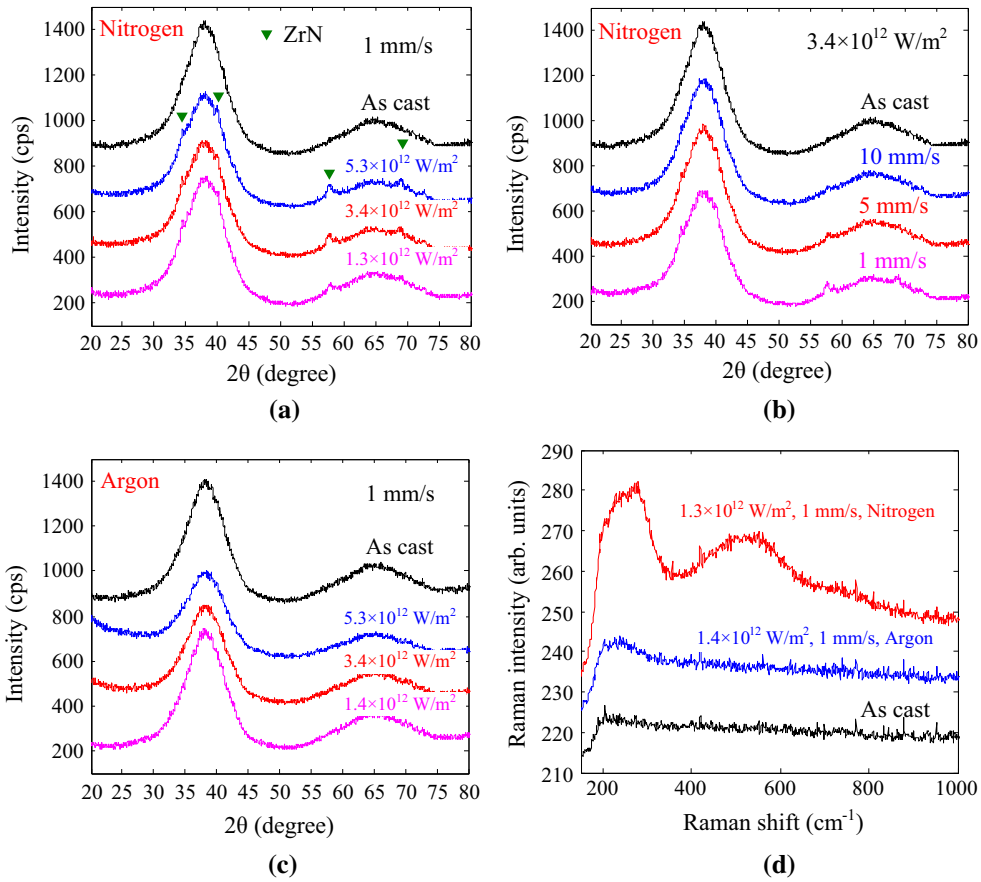

Fig. 4 **a–c** XRD patterns and **d** micro-Raman spectra obtained in the *multi-line* laser scanned regions. Detailed experimental conditions are inserted in each figure

scans healed the cracks formed in previous scans. XRD and Raman results indicated that the promoted crack formation in nitrogen gas resulted from the formation of ZrN.

Acknowledgments H.H. is an International Research Fellow of the Japan Society for the Promotion of Science (JSPS). This study has been financially supported by Grant-in-Aid for JSPS Fellows (Grant No. 26-04048).

References

1. S. Pauly, L. Lober, R. Petters, M. Stoica, S. Scudino, U. Kuhn, J. Eckert, Mater. Today **16**(1–2), 37–41 (2013)
2. H.Y. Jung, S.J. Choi, K.G. Prashanth, M. Stoica, S. Scudino, S. Yi, U. Kuhn, D.H. Kim, K.B. Kim, J. Eckert, Mater. Design **86**, 703–708 (2015)
3. X.P. Li, C.W. Kang, H. Huang, L.C. Zhang, T.B. Sercombe, Mat. Sci. Eng. A-Struct. **606**, 370–379 (2014)
4. B. Li, Z.Y. Li, J.G. Xiong, L. Xing, D. Wang, Y. Li, J. Alloy. Compd. **413**(1–2), 118–121 (2006)
5. G. Wang, Y.J. Huang, M. Shagiev, J. Shen, Mat. Sci. Eng. A-Struct. **541**, 33–37 (2012)
6. T.M. Yue, Y.P. Su, H.O. Yang, Mater. Lett. **61**(1), 209–212 (2007)
7. Y.Y. Zhu, Z.G. Li, R.F. Li, M. Li, X.L. Daze, K. Feng, Y.X. Wu, Appl. Surf. Sci. **280**, 50–54 (2013)
8. Z. Liu, K.C. Chan, L. Liu, S.F. Guo, Mater. Lett. **82**, 67–70 (2012)
9. M.Q. Jiang, Y.P. Wei, G. Wilde, L.H. Dai, Appl. Phys. Lett. **106**(2), 021904 (2015)
10. Y. Liu, M.Q. Jiang, G.W. Yang, Y.J. Guan, L.H. Dai, Appl. Phys. Lett. **99**(19), 191902 (2011)
11. W. Zhang, G. Cheng, X.D. Hui, Q. Feng, Appl. Phys. A-Mater. **115**(4), 1451–1455 (2014)
12. X.Y. Ye, Y.C. Shin, Surf. Coat. Tech. **239**, 34–40 (2014)
13. X.Y. Ye, H. Bae, Y.C. Shin, L.A. Stanciu, Metall. Mater. Trans. A **46A**(9), 4316–4325 (2015)
14. B.Q. Chen, Y. Li, M. Yi, R. Li, S.J. Pang, H. Wang, T. Zhang, Scripta Mater. **66**(12), 1057–1060 (2012)
15. S. Katakam, J.Y. Hwang, H. Vora, S.P. Harimkar, R. Banerjee, N.B. Dahotre, Scripta Mater. **66**(8), 538–541 (2012)
16. S. Ningshen, U.K. Mudali, R. Krishnan, B. Raj, Surf. Coat. Tech. **205**(15), 3961–3966 (2011)
17. E. Williams, E.B. Brousseau, J. Mater. Process. Tech. **232**, 34–42 (2016)
18. J.Y. Li, Y. Sun, Y. Tan, F.M. Xu, X.L. Shi, N. Ren, Chem. Eng. J. **144**(1), 149–152 (2008)
19. Y.S. Touloukian, R.K. Kirby, R.E. Taylor, P.D. Desai, *Thermo-physical properties of matter, volume 12-thermal exapnsion-metallic elements and alloys* (Plenum Press, New York, 1975)
20. M.Q. Jiang, M. Naderi, Y.J. Wang, M. Peterlechner, X.F. Liu, F. Zeng, F. Jiang, L.H. Dai, G. Wilde, AIP Adv. **5**(12), 127133 (2015)